NASA Technical Memorandum 82785

Identification of Multivariable High Performance Turbofan Engine Dynamics From Closed Loop Data

Walter Merrill
Lewis Research Center
Cleveland, Ohio

Prepared for the
Sixth IFAC Symposium on Identification
and System Parameter Estimation
sponsored by the IFAC Technical Committee on
Applications and the IFAC Theory Committee
Washington, D.C., June 7-11, 1982

NASA

IDENTIFICATION OF MULTIVARIABLE HIGH PERFORMANCE TURBOFAN ENGINE DYNAMICS FROM CLOSED LOOP DATA

by Walter Merrill

National Aeronautics and Space Administration
Lewis Research Center
Cleveland, Ohio 44135

Abstract. The multivariable Instrumental Variable/Approximate Maximum Likelihood (IV/AML) method of recursive time-series analysis is used to identify the multivariable (four inputs-three outputs) dynamics of the Pratt and Whitney F100 engine. A detailed non-linear engine simulation is used to determine linear engine model structures and parameters at an operating point using open loop data. Also, the IV/AML method is used in a direct identification mode to identify models from actual closed loop engine test data. Models identified from simulated and test data are compared to determine a final model structure and parameterization that can predict engine response for a wide class of inputs. The ability of the IV/AML algorithm to identify useful dynamic models from engine test data is assessed.

Keywords. Multivariable identification; Jet engine; Closed loop data; Instrumental variable/approximate maximum likelihood

E-1120

INTRODUCTION

A typical engine control design cycle consists of developing a dynamic engine simulation from steady-state component performance data, designing a control based upon this simulation, and then testing and modifying the control in an engine test cell to meet performance requirements. This design cycle has been successful for state-of-the-art engines. However, for more advanced multivariable engines that exhibit strong variable interactions, this procedure will result in substantial trial and error modification of the control during the testing phase. One method to automate the design process and reduce control modification testing and development cost would be to identify accurate dynamic models directly from the closed loop test data. These identified models would then be used in conjunction with a synthesis procedure to systematically refine the control. Recent advances in closed loop identifiability (Ref. 1) present a methodology for this direct identification of engine model dynamics from closed loop test data. This paper describes the application of the IV/AML identification method (Ref. 2) to simulated and actual closed loop F100 engine data (Ref. 3). This study was undertaken to determine if useful dynamic engine models could be identified directly from closed loop engine test data.

Recently, some gas turbine models have been identified. In Refs. 4 and 5 a single input state-space model was obtained by a time series method from simulated input-output data. In Ref. 6 a nonlinear filtering technique was used to estimate system parameters from multiple input simulated engine data. In Ref. 8 a two input engine model was determined from open loop data analysis using the "Method of Models." Later the model form of Ref. 8 was applied to condition monitoring for a single input engine (Ref. 9). In Ref. 10 a single input engine model was determined from closed loop flight data using a maximum likelihood parameter search of dynamic engine simulation parameters. It was assumed that there was no process noise. In Ref. 11 a two input automotive gas turbine model was identified from open loop engine frequency and step response data. The two data types were used in concert to fix the model structure and to fit the model parameters.

In this report the IV/AML method is applied to both simulated and actual closed loop test multiple input data. The IV/AML method is an output error identification method and was implemented in a combined iterative/recursive form. As yet, the IV/AML method has not seen wide application to many physical processes, and, until now, the method has not been applied either to gas turbine engine data or to closed loop data. The test data studied in this report contains both measurement and process noise. The available closed loop engine test data records are each comprised of only 200 sample points. Since this is a relatively low number of sample points per operating record, the IV/AML method was

selected for use because Monte Carlo tests have shown the method to exhibit reasonable convergence for a small number of samples (Ref. 2).

This report begins with a brief description of the IV/AML method and its application to engine model identification. Next, an engine model structure is developed and applied to simulation and test data.

THE IV/AML IDENTIFICATION METHOD

The multivariable IV/AML method is the time series analysis tool used in this study. Monte Carlo simulation has shown the method to be an asymptotically efficient identification tool. A complete descripton of the Refined IV/AML method is given in Ref. 2. Briefly, the model is written as:

$$A(z^{-1})x_k = B(z^{-1})u_k \tag{1a}$$

$$C(z^{-1})\xi_k = D(z^{-1})e_k \tag{1b}$$

$$y_k = x_k + \xi_k \tag{1c}$$

where z^{-1} is the backward shift operator. The vectors $y_k \epsilon R^{n_y}$ and $u_k \epsilon R^{n_u}$ are known and represent the noisy output and deterministic input, respectively. The vector x_k is the deterministic part of y_k and ξ_k models the effects of unmeasureable disturbances and measurement noise. The vector $e_k \epsilon R^{n_y}$ satisfies:

$$E\{e_k\} = 0;\ E\{e_j e_k^T\} = Q\delta_{jk};\ E\{e_j u_k^T\} = 0 \tag{2}$$

The polynomial matrices A, B, C and D are defined as:

$$A = I + \sum_{i=1}^{n} A_i z^{-i}$$

$$B = B_0 + \sum_{i=1}^{n} B_i z^{-i} \tag{3}$$

$$C = I + \sum_{i=1}^{n} C_i z^{-i}$$

$$D = I + \sum_{i=1}^{n} D_i z^{-i}$$

where A_i, B_i, C_i and D_i are real matrices. The algorithmic structure of the iterative/recursive version of the IV/AML method is given in Fig. 1. Here the auxiliary system model is updated iteratively after a complete passage through the data during which the model is maintained at the previous iteration value, $\hat{\theta}_{a_T}$. The noise model, however, is updated recursively. Model updates are determined by the IV algorithm and the AML algorithm blocks of Fig. 1. These two algorithms have the same basic structure and represent iterative solutions to the necessary conditions for maximizing a log likelihood function of the observations. The algorithms basically update the model parameters as a function of output error and estimated parameter uncertainty. Prefiltering, which is used in a "refined" IV/AML procedure, can yield estimates with improved statistical efficiency. Prefiltering was not used in this study, however, due to the additional computational complexity and the satisfactory operation of the "standard" IV/AML approach. The noise covariance was estimated by:

$$\hat{Q}_k = \hat{Q}_{k-1} + \frac{1}{k}\left[e_k e_k^T - \hat{Q}_{k-1}\right] \tag{4}$$

When applying the IV/AML method of Fig. 1 to the engine data, usually six iterative passes through the data were taken. Initial parameter values for the system and for the noise covariance were determined from open loop simulation data. Values for the initial asymptotic parameter covariance matrices, $\hat{P}$ for the parameters of θ_a and $\hat{R}$ for the θ_c, were selected as:

$$\hat{P}_0 = \mu I$$

$$\hat{R}_0 = \mu_R I \tag{5}$$

where $\mu = \mu_R$ in general and μ is selected as approximately 100 to 1000 times larger than the diagonal elements of Q. Once estimates of θ_a, θ_c, and Q were obtained in one test, they were often used as initial values in subsequent tests. However, during each test, $\hat{Q}$ was normally held constant during the iterations 1-4 and 6, and updated during iteration 5. Eigenvalues of $\hat{A}$, $\hat{C}$, and $\hat{D}$ were calculated at the start of each iteration to insure stable algorithm operation. Also, comparison of eigenvalues from one iteration to the next is a good indicator of algorithm performance. For example, the movement of one eigenvalue of $\hat{A}$ toward the stability bound indicates that the algorithm is "getting lost" or that an incorrect model structure has been chosen. Also, norms $\hat{P}_k$ and $\hat{R}_k$ were calculated at each iteration as a measure of convergence.

ENGINE MODEL

The Pratt and Whitney F100 engine (Ref. 3) is a twin-spool low-bypass ratio afterburning turbofan. Four controlled variables are considered: main fuel flow (WF), exhaust nozzle area (AJ), compressor (fan) inlet variable guide vanes (CIVV), and the rear compressor variable guide vanes (RCVV). Three output variables are considered: engine fan speed (N1), engine compressor speed (N2), and augmentor entrance pressure (PT6). The engine speeds are indicative of the dynamic response of the engine while PT6 is closely related to engine thrust. Globally the engine is modeled as

$$\begin{aligned} \dot{x} &= f(x,u,ALT,MN) \\ y &= g(x,u,ALT,MN) \end{aligned} \tag{6}$$

where x is the state vector, u is the control vector and y is the output vector. Engine operation is also dependent upon environmental variables altitude (ALT) and Mach number (MN). An engine operating point is defined as

$$\begin{aligned} f(x_{ss},u_{ss},ALT,MN) &= 0 \\ g(x_{ss},u_{ss},ALT,MN) &= y_{ss} \end{aligned} \tag{7}$$

A third order behavioral model relating the engine outputs to the primary control variables WF and AJ was developed in Ref. 12 and is given as

$$\dot{x} = \begin{bmatrix} -1/\tau_1 & C_{HL} & C_{PL} \\ 0 & -1/\tau_2 & 0 \\ 0 & C_{LP} & -1/\tau_p \end{bmatrix} x + \begin{bmatrix} b_{FL} & 0 \\ b_{FH} & 0 \\ 0 & b_{AP} \end{bmatrix} u \tag{8}$$

This model represents linearized behavior in a small rgion about an operating point. Including CIVV and RCVV and writing in the form of (1), the behavioral model becomes

$$\left(I + A_1 z^{-1}\right) x_k = B_1 z^{-1} u_k \tag{9}$$

where x = (N1, N2, PT6) and u = (WF, AJ, CIVV, RCVV).

Simulation Application

The IV/AML method using the model of (9) was initially applied to open loop SISO digitally simulated engine data. These data were obtained for an ALT = 10 000 ft, MN = 0.9 intermediate power operating point. Two data sets were generated in the following manner. All controls were held constant at their steady-state operating point values except for WF in the first case:

$$WF = WF_{ss}(1 + 0.03\,\gamma_k) \tag{10}$$

and AJ in the second case

$$AJ = AJ_{ss}(1 + 0.03\,\gamma_k) \tag{11}$$

where γ_k is Gaussian noise with

$$\begin{aligned} E\{\gamma_k\} &= 0 \\ E\{\gamma_k^2\} &= 1 \end{aligned} \tag{12}$$

Equations (10) and (11) represent ±3 percent variations about the nominal operating point to insure linear operation. In both cases the sampling rate was $T = 0.01$ sec. From these two data sets an initial estimate of A_1 was obtained as

$$A_1 = \begin{pmatrix} -0.85 & 0 & 0 \\ 0 & -0.96 & 0 \\ 0.615 & 0 & -0.4 \end{pmatrix} \tag{13}$$

This corresponds to continuous eigenvalues of -16, -4, and -90. This information was used as a starting point in MIMO identification test.

A random input emphasizes identification at all frequencies. However, the frequency range of engine operation is practically limited by actuator and engine hardware to about 20 radians/sec. Thus a set of inputs was chosen, somewhat arbitrarily, for a MIMO test that empahsized this more realistic frequency range. Here

$$u_k = u_{ss}(1 + 0.03\Delta u_k) \tag{14}$$

and

$$\Delta u_k = \begin{bmatrix} (\sin(0.1kT) + \cos(5kT + 2) \\ (\sin(0.2kT) + \cos(7kT + 4) \\ (\sin(0.3kT) + \cos(5kT) \\ (\cos(0.4kT - 4) - \cos(10kT) \end{bmatrix} \tag{15}$$

Also the sampling interval was selected to be $T = 0.05$ sec to correspond to subsequent tests which used actual test data recorded at $T = 0.05$ sec. Four hundred data points ($K = 400$) for each test were recorded. The IV/AML method was applied and the results are given as model 1 in Table 1. The average percent error per point was calculated from the outputs as

$$\text{Error}_i = \frac{\sqrt{\sum_{k=1}^{K} \hat{\xi}_{ki}^2}}{100\ K\ \underset{k}{\text{Max}}\ |y_{ki}|} \qquad (16)$$

and is given in Table 1 also. For model 1 each output has less than 0.6 percent error per point on the average which is a good fit of the data. An additional element in A_1 was found to be required to satisfactorily model PT6.

The noise model (see Fig. 1) was found to be close to the auxiliary model. Thus, the number of parameters could be reduced by constraining $C_1 = A_1$. However, this was not pursued as large improvements in model accuracy were not anticipated by enforcing this constraint. Additionally, initial identification tests showed the eigenvalues of the D matrix to be beyond the frequency range of interest. Therefore, the D matrix was constrained to be $D = I$.

The noise covariance, Q, is also given in Fig. 1. Since Q did not change substantially from model 1 to model 2, subsequent models were identified using the Q of model 2. Periodic updates of the value of Q in subsequent models showed no large variation in Q.

Model 1 of Table 1 was used to predict engine behavior based upon actual closed loop engine test data. This is described in the next section.

Test Data Application

The F100 engine was tested in the Lewis Research Center altitude test facilty to evaluate the F100 Multivariable Control (MVC) law (Refs. 2 and 3). During the same test period the "Bill of Material" (BOM) control was also evaluated as a baseline/backup control model. Thus, there are a variety of closed loop operating records obtained throughout the flight envelope with a number of different power input requests. The two multivariable data sets used in this report were recorded at an ALT = 10 000 ft, MN = 0.9 condition as the power request was varied (step change) in a small (hopefully linear) range about intermediate engine power. One set corresponds to an MVC control test, the other to a BOM test. Data were sampled at $T = 0.05$ sec for a 10-second transient, which yields $K = 200$ points for each record in the data sets.

The BOM and MVC control structures, linearized at an operating point, correspond to the structure of Fig. 2. The reference point and control blocks are different however for the two controls. The structure of Fig. 2 is exactly the structure given in Ref. 1. Since each control structure is fixed at a given operating point, strong system identifiabilty can be guaranteed if

$$\text{Rank}\begin{bmatrix} I & 0 \\ F & L \end{bmatrix} = n_u + n_y \qquad (17)$$

Or in other words, if

$$\det[L] \neq 0 \qquad (18)$$

The BOM and MVC reference point schedules do exhibit the characteristic of (18), therefore a direct identification approach, such as IV/AML, can be successfully applied to the closed loop input/output data sets recorded in the Lewis test facility.

Sensor instrumentation for the input and output variables of interest is summarized in Table 2. In each case sensor dynamics are beyond the 20 radians/sec frequency range. Thus, sensor dynamics were initially ignored in the identification tests. Ambient noise statistics were obtained during steady-state engine operation. Standard deviations were calculated at the operating point for the sensed values. Signal to noise ratios (SNR's) were estimated based upon these ambient noise levels and the deviations of the various signals from their operating point values. These SNR's are included in Table 2. In each case the SNR's show the level of noise to be small relative to the signal. Therefore, the identification results should be quite consistent and accurate.

Normalized WF from the BOM and MVC control tests is shown in Fig. 3. This is typical of the engine inputs in these tests. Power spectrum analysis of these inputs shows a slightly higher frequency component in the MVC inputs, although more total power is contained in the BOM inputs. However, for both the BOM and MVC inputs most of the power is concentrated below 6 radians/sec.

The control inputs of Fig. 3 were used in conjunction with the identified model 1 to predict engine output. Comparing the predicted outputs of model 1 with the actual outputs, it was apparent that model 1 was unacceptable. No output was predicted well for either BOM or MVC data. Figure 4 is typical of the comparison. Slight discrepancies between simulation and test data cannot account for large discrepancies between predicted and actual outputs.

To investigate this further the IV/AML method was applied directly to the closed loop test data producing models 2 and 3. Model 1 was used as a starting point. As illustrated in Fig. 5, model 3 accurately reproduces the data, from which it was generated (BOM). Model 2 results are similar. In fact, Fig. 1 shows the error of

all the outputs for models 1, 2 and 3 to be less than 1 percent. However, comparing parameters for models 1, 2 and 3 (see Table 1) it can be seen that while A_1 remains essentially unchanged elements of B_1 do change substantially. This implies a slightly overparameterized model structure which does account for the inability of model 1 to predict BOM and MVC engine data. To determine which elements should be eliminated to remove the overparameterization, the following procedure was adopted.

First, a reasonably accurate initial model is assumed. In this case, models 2 and 3 were used. An initial covariance matrix

$$P_o = \text{diag}(p_{oi}) \tag{19}$$

is chosen where the p_{oi} are small to indicate small uncertainty in the model parameters. In the engine example

$$P_o = 10^{-7} I \tag{20}$$

was used. Next, the IV/AML method is applied for only a single iteration to data for which the model is overparameterized. The method now will be most sensitive to removing the uncertainty inherent in the extra parameters. Now, the diagonal elements of P_1 which correspond to accurate parameters will not change. However, the diagonal elements of P_1, p_{1i}, which correspond to extra parameters will change significantly. Thus, if

$$|p_{1i} - p_{oi}| > \epsilon p_{oi} \tag{21}$$

where ϵ is a positive threshold, the corresponding parameter a_i can be set to zero. The threshold was selected as

$$\epsilon = 0.05 \tag{22}$$

for the engine data.

Three elements of P_1 satisfied (21) for both the MVC and BOM data. The corresponding parameters were eliminated and this new structure applied to the simulation data generated by the inputs of (14) and (15). The resultant IV/AML identified model is given as model 4 in Table 1. A comparison of average fit error is quite comparable to model 1 with full B_1 and, in fact, shows improvement in the PT6 comparison.

Note that the eigenvalue associated with PT6 in model 4 represents a frequency of approximately 25 radians/sec which is slightly greater than the 20 radians/sec natural frequency of the PT6 sensor. Obviously, the PT6 sensor dynamics can no longer be competely ignored in the interpretation of the results. Additionally, since one mode models the sensor dynamics, a second mode may be required to model the PT6 engine mode. This was not pursued at this time however.

When used to predict BOM and MVC output data, model 4 was still unsatisfactory. Model 4 did predict N1(MVC), N2(MVC), and N2(BOM). However, N1(BOM) and especially PT6 for both data sets were not predicted well. The error in PT6 is somewhat expected from sensor and input bandwidth considerations. The N1(BOM) error was not expected however. Figure 6 compares predicted N1 data using model 4 to actual closed loop N1(BOM) data. Model 4 predicted N1 grossly follows the trend of the simulated data. Thus, it appears that the dynamic portion of model 4 is correct. However, there must then be large discrepancies in some of the model 4 gain terms. These discrepancies are somewhat perplexing since model 4 predicted N1(MVC) but not N1(BOM).

Recall, however, that the BOM inputs are larger in magnitude than the MVC inputs, and that model 4 represents linearized dynamics. Thus, some nonlinear effects may be inherent in the BOM data. This explanation is not entirely satisfactory since N2(BOM) and N2(MVC) were both predicted. Further work to resolve this problem is required. The IV/AML identification method was again utilized to further refine the model parameters for the structure of model 4 using the two sets of experimental closed loop data. The purpose of this final iteration is to identify a single model that can accurately predict both sets of engine test data and, hopefully, simulation data as well.

Again model 4 was used as an initial condition in the IV/AML method applied to the BOM and MVC data. Models 5 and 6 of Table 1 resulted. Both models 5 and 6 fit their respective data sets quite well. Figures 6 to 8, for example, show a good fit of the BOM data by outputs predicted using model 5. Similar comparisons to MVC data were obtained using model 6. More importantly, when the BOM model 5 is used to predict the MVC data, the comparison given in Figs. 9 to 11 is quite reasonable. Thus, model 5 (or equivalently model 6) represents a model which predicts a class of inputs and can be used with confidence in a control design procedure.

CONCLUSIONS

The IV/AML method was applied to both open loop simulation and closed loop test data of an F100 turbofan engine. The method accurately and consistently identified models from both the simulation and test data. Due to the structure of the BOM and MVC control laws, the engine model is strongly system identifiable and consequently a direct identification approach was used on the closed loop data.

A third order model structure was derived and found to be overparameterized. Three parameters were eliminated by sensitivity considerations. The simplified structure was found acceptable for fitting both simulation and test data. Test model accuracy is limited to 6 radians/sec since spectral analysis of the inputs shows limited signal strength above this frequency.

Also, identification results indicate that PT6 related model parameter accuracy is further limited by sensor bandwidth and that an additional dynamic mode is required to faithfully model PT6.

Comparisons showed that models identified from simulated data generally predicted N1(MVC), N2(MVC), and N2(BOM) test response adequately. However, predictions of PT6(MVC) and PT6(BOM were poor and N1(BOM) showed some discrepancies in dynamics. The PT6 differences are attributed to the low frequency content of the test input signals (<6 radians/sec), the bandwidth of the sensor, and the high frequency nature of the PT6 mode. However, the difference in N1 is attributable to a difference in simulated versus actual engine performance. This conclusion is accurately portrayed in a comparison of identified models.

Finally, a simplified model determined from BOM data accurately predicted not only BOM but also MVC test response data. This ability to predict engine performance for a class of inputs generates confidence in controls designated from this model. Thus, it is concluded that useful dynamic engine models can be obtained from closed loop test data using the IV/AML identification method. This identification technique, then, represents the first step in an automated engine control design process.

REFERENCES

Soderstrom, T.; Ljung, L.; and Gustavsson, I.: Identifiability Conditions for Linear Multivariable Systems Operating Under Feedback. IEEE Trans. of Autom. Control, Vol. AC-21, No. 6, Dec. 1976, pp. 837-840.

Jakeman, A.; and Young, P.: Refined Instrumental Variable Methods of Recursive Time-Series Analysis - Part II, Multivariable Systems. Int. J. Control, Vol. 29, No. 4, 1979, pp. 624-644.

Lehtinen, F. K. B.; Costakis, W. G.; Soeder, J. F.; and Seldner, K.: Altitude Test of a Multivariable Control System for the F100 Engine. NASA TP (to be published).

Merrill, W.; and Leininger, G.: Identification and Dual Adaptive Control of a Turbojet Engine. Int. J. Control, Vol. 34, No. 3, Sept. 1981, pp. 529-546.

Merrill, W. C.: An Application of Modern Control Theory to Jet Propulsion Systems. NASA TM X-71726, 1975.

Michael, G. J.; and Farrar, F. A.: Identification of Multivariable Gas Turbine Dynamics from Stochastic Input-Output Data. UARL-R941620-3, United Aircraft, 1975 (AD-A006277).

DeHoff, R. L.; and Hall, W. E.: System Identification Principles Applied to Multivariable Control Synthesis of the F100 Turbofan Engine. Joint Automatic Control Conference, Proceedings, Vol. 2. IEEE. 1977, pp. 1007-1012.

Rault, A.; Richalet, J.; Bardot, A.; Sargenton, J. P.: Identification and Modeling of a Jet Engine. Presented at IFAC Symposium on Digital Simulation of Continuous Processes (Gyor, Hungary), Sept. 6-10, 1971.

Baskiotis, C.; Raymond, J.; and Rault, A.: Parameter Identification and Discriminent Analysis for Jet Engine Mechanical State Diagnosis. Conf. on Decision and Control, 18th, Ft. Lauderdale, FL, Dec. 1979, Proceedings, Vol. 2, IEEE, 1979, pp. 648-650.

DeHoff, R. L.: Identification of a STOL Propulsion Plant Model from Flight Data. J. Guidance and Control, Vol. 2, No. 3, May-June 1979, pp. 235-240.

Wellsted, P. E.; and Nuske, D. J.: Identification of an Automotive Gas Turbine. Int. J. Con- trol, Vol. 24, No. 3, Part I, Frequency Response Estimation, pp. 297-309; Part II, Parameter Fitting, pp. 311-324.

DeHoff, R. L.; Hall, W. E., Jr.; Adams, R. J.; and Gupta, N. K.: F100 Multivariable Control Synthesis Program. Vols. I and II, AFAPL-TR-77-35, June 1977. (AD-A052420 and AD-A052346.)

TABLE 1 Identified Model Parameter Values

Model	Model data source	Number of data points	A_1	B_1	C_1	$Qx10^5$	Percent error
1	Simulation	400	-0.840 0 0 0 -.858 0 .382 -.120 -.396	0.0405 0.0395 0.0005 -0.0032 .0235 .0102 .0006 .0029 .2133 -.3362 -.0026 -.0318	-0.970 0 0 0 -.978 0 .092 0 -.977	0.225 0.056 -0.314 .056 .040 .171 -.314 .171 4.486	0.421 .489 .581
2	MVC test	200	-0.865 0 0 0 -.801 0 .368 -.124 -.344	0.0405 0.0442 0.0029 -0.0002 .0318 .0088 -.0023 -.0002 .1937 -.3284 -.0672 -.0022	-0.951 0 0 0 -.960 0 .108 0 -.971	0.189 0.046 0.021 .046 .017 .064 .021 .064 2.692	0.431 .264 .894
3	BOM test	200	-0.850 0 0 0 -.836 0 .379 -.119 -.346	0.380 0.0405 0.0017 -0.0003 .0324 .0112 .0012 -.0004 .2092 -.3343 -.0221 .0155	-0.982 0 0 0 -.971 0 .086 0 -.974	0.189 0.046 0.021 .046 .017 .064 .021 .064 2.692	0.117 .185 .524
4	Simulation	400	-0.700 0 0 0 -.859 0 .264 -.189 -.293	0.0631 0.0769 -0.0032 0 .0245 .0110 0 0 .1862 -.5070 -.0338 -.0415	-0.974 0 0 0 -.988 0 .060 0 -.960	Same as above	0.550 .469 .375
5	BOM test	200	-0.670 0 0 0 -.818 0 .266 -.189 -.283	0.0378 0.0465 -0.0095 0 .0290 .0066 0 0 .1701 -.4981 -.0474 .0116	-0.982 0 0 0 -.973 0 .048 0 -.965	Same as above	0.115 .205 .528
6	MVC test	200	-0.728 0 0 0 -.808 0 .255 -.194 -.291	0.0508 0.0805 -0.0028 0 .3030 .0193 0 0 .1801 .4989 -.0842 -.0034	-0.951 0 0 0 -.964 0 .059 0 -.958	Same as above	0.425 .275 .754

TABLE 2 Engine Instrumentation

Sensed variable	Symbol	Type	Time constant, sec	SNR_{MVC}	SNR_{BOM}
Fan speed	N1	Tachometer	0.03	23.8	152
Compressor speed	N2	Tachometer	.05	16.97	80
Augmentor/exhaust pressure	PT6	Strain gauge	.05	10.78	116.8
Main burner fuel flow	WF	Flow meter	.02	6.91	22.8
Jet area servo stroke	AJ	Position transducer	.02	24.54	571
Inlet guide vane deflection	CIVV	Servo feedback	.02	35.15	206
Compressor vane deflection	RCVV	Servo feedback	.02	14.86	105.9

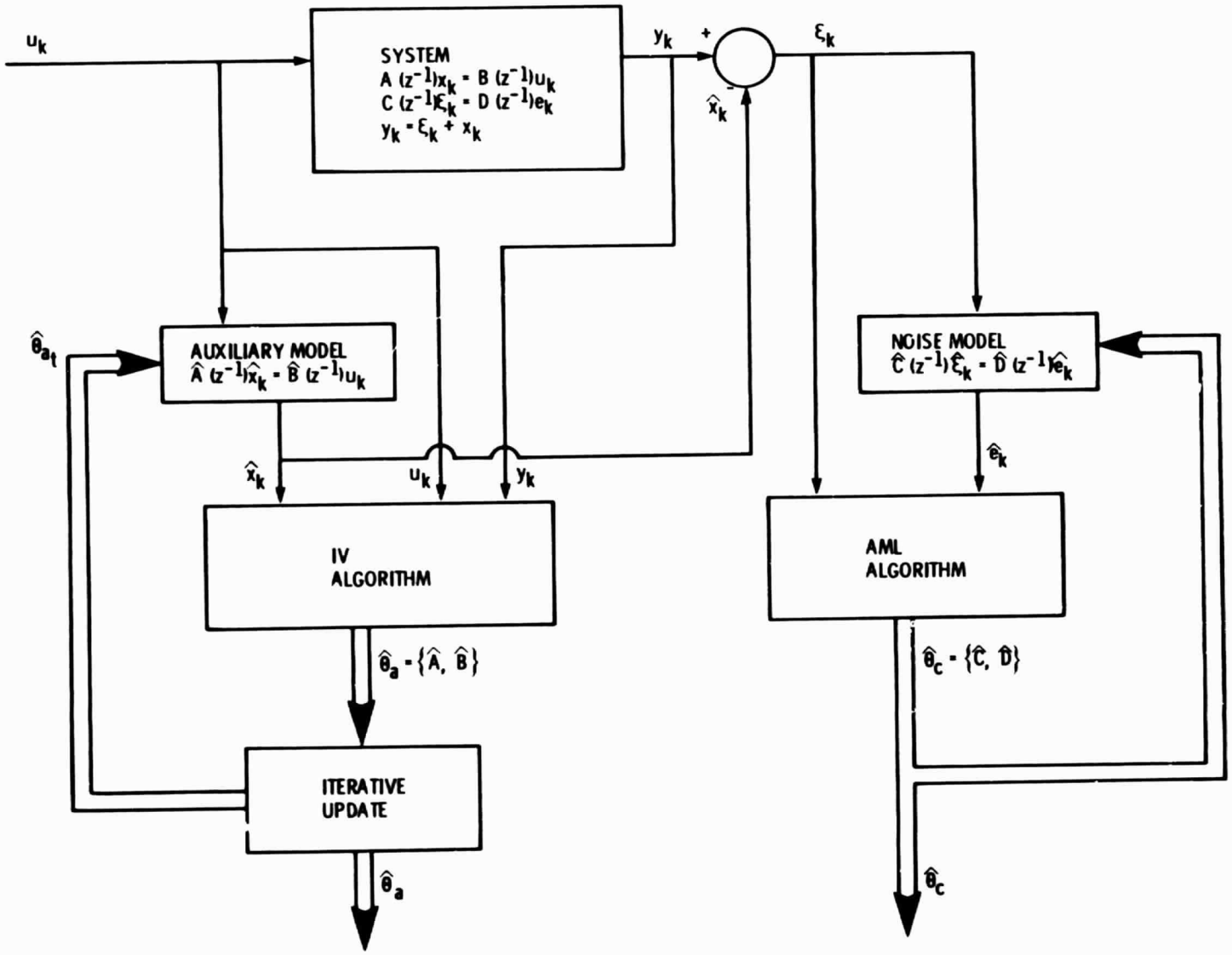

Figure 1. - Iterative IV/AML version structure.

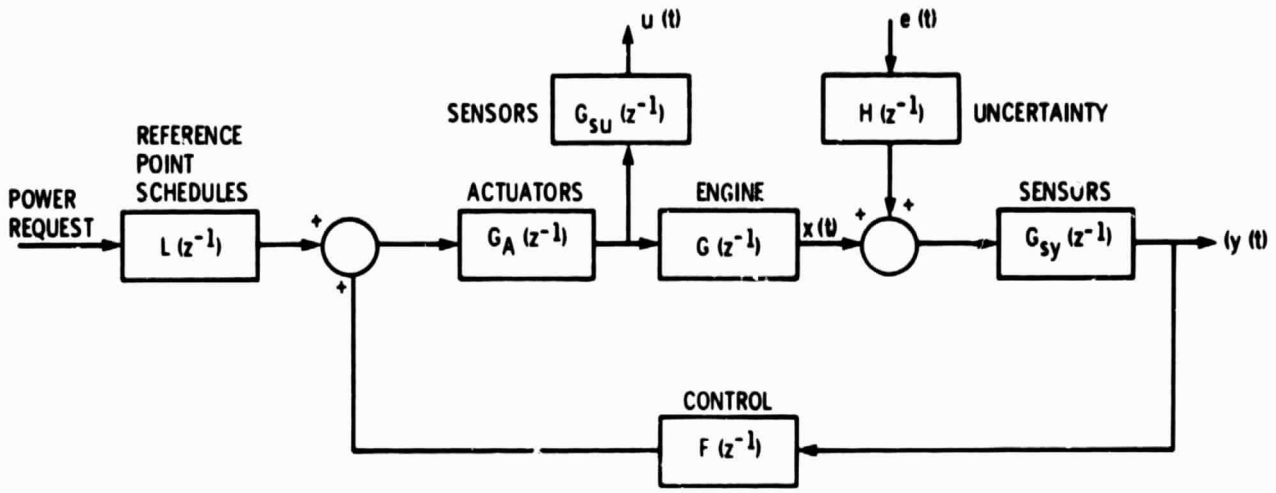

Figure 2. - Engine control structure.

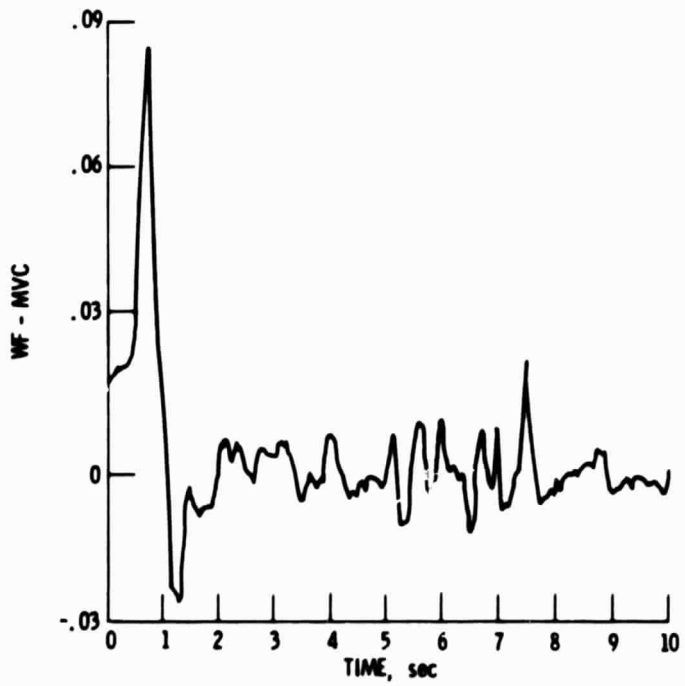

Figure 3. - Engine inputs; WF.

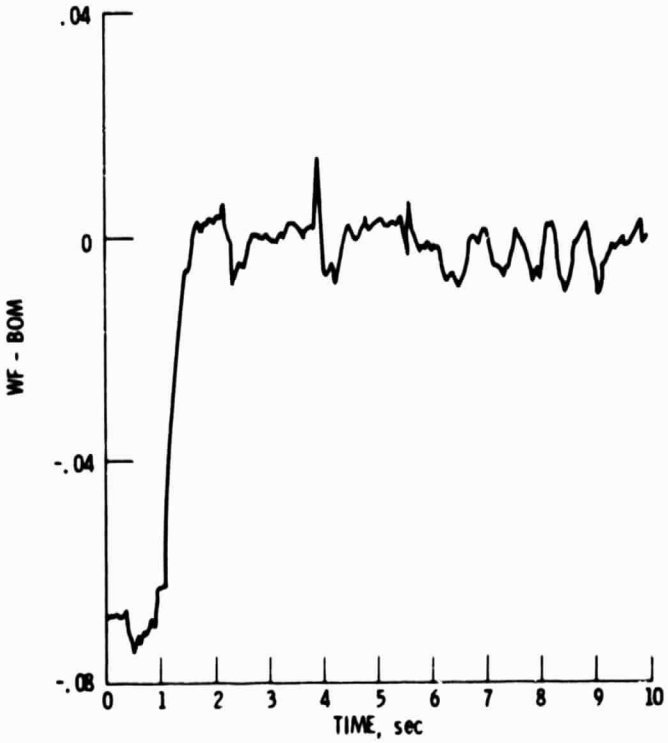

Figure 3. Continued.

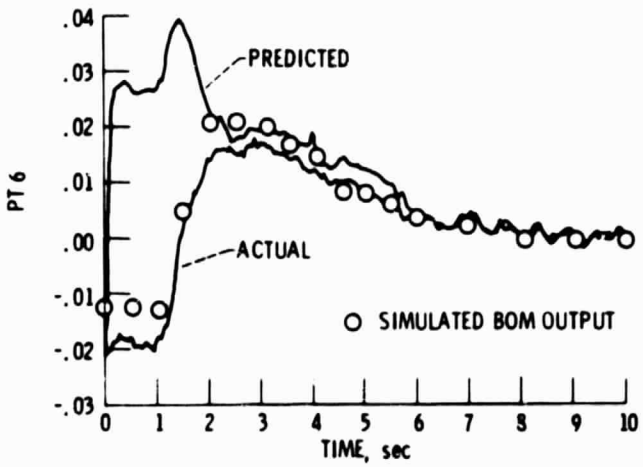

Figure 4. - Comparison of actual BOM output with a simulated BOM output and an output predicted by model obtained from simulation data - unconstrained B_1.

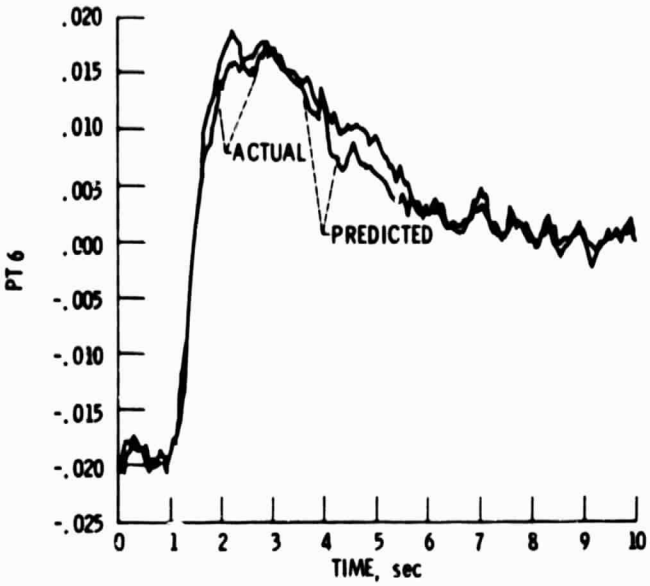

Figure 5. - Comparison of actual BOM output with output predicted by model 3 obtained from BOM data - unconstrained B_1.

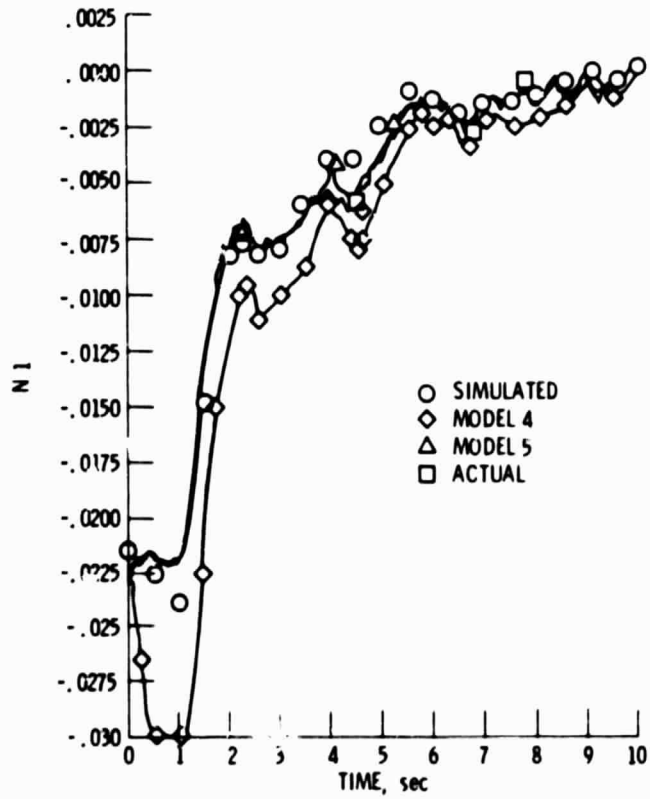

Figure 6. - Comparison of actual BOM output with a simulated BOM output and outputs predicted by models 4 and 5.

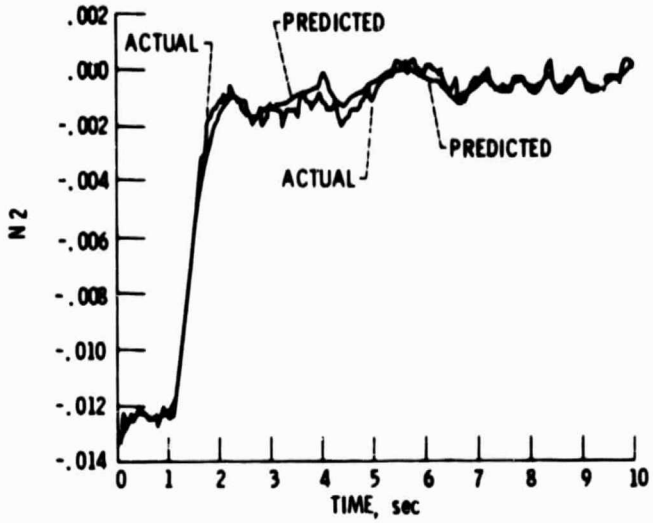

Figure 7. - Comparison of actual BOM output with output predicted by model 5 obtained from BOM data - constrained B_1.

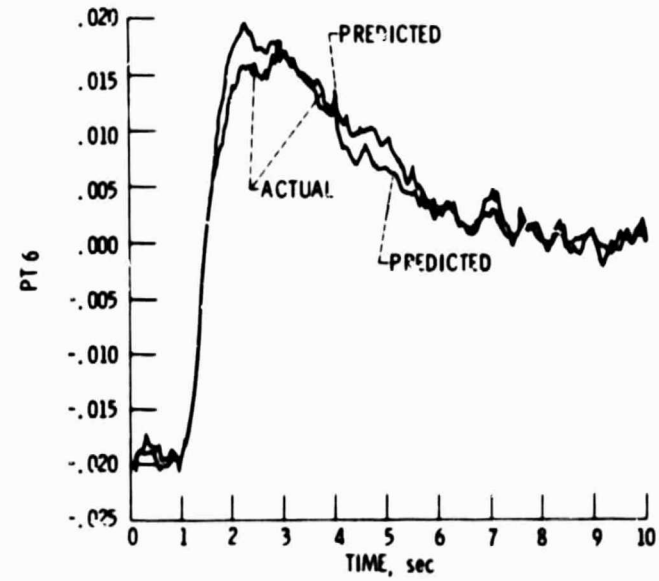

Figure 8. - Comparison of actual BOM output with output predicted by model 5 obtained from BOM data - constrained B_1.

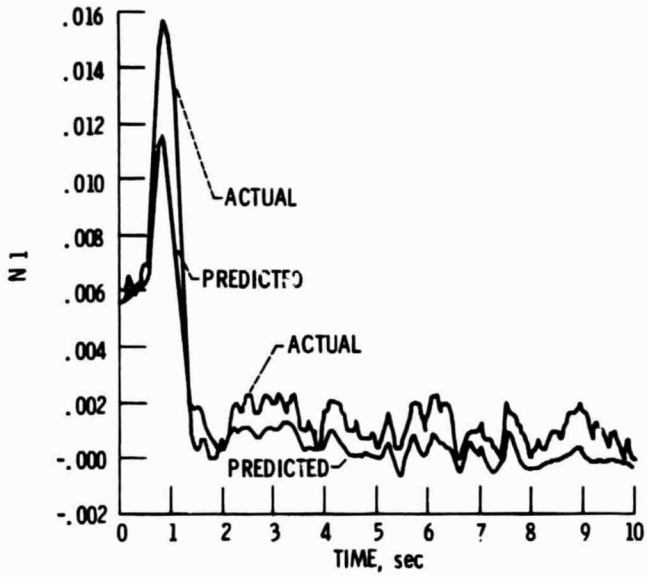

Figure 9. - Comparison of actual MVC output with output predicted by model 5 obtained from BOM data - constrained B_1.

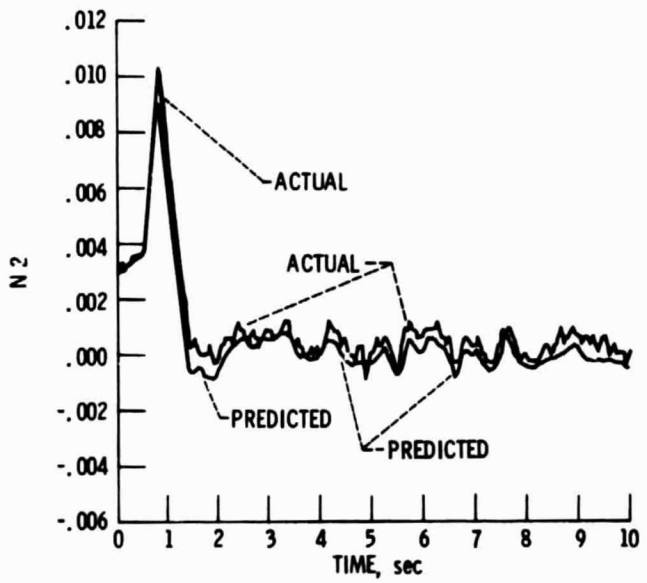

Figure 10. - Comparison of actual MVC output with output predicted by model 5 obtained from BOM data - constrained B_1.

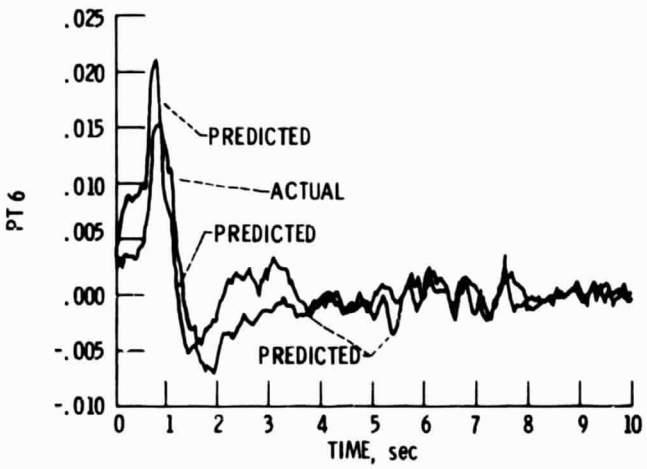

Figure 11. - Comparison of actual MVC output with output predicted by model 5 obtained from BOM data - constrained B_1.